Sixth International Conference on Sustainable Construction Materials and Technologies. https://www.scmt-conferences.com/proceedings

LINKING MICROSTRUCTURE ASPECTS AND MECHANICAL BEHAVIOUR OF WOOL REINFORCED COMPOSITES

Alessandro P. Fantilli[1], Daria Jóźwiak-Niedźwiedzka[2]
Aneta Antolik[2], Piotr Denis[2]

[1] *DISEG, Politecnico di Torino, Corso Duca degli Abruzzi 24, 10129 Torino, Italy, alessandro.fantilli@polito.it*
[2] *Institute of Fundamental Technological Research, Polish Academy of Sciences, Pawińskiego 5b, 02-106 Warsaw, Poland, djozwiak@ippt.pan.pl, aantolik@ippt.pan.pl, pdenis@ippt.pan.pl*

ABSTRACT

The necessity of tailoring more environmentally friendly materials has prompted researchers and practitioners to explore new and more sustainable components for cement-based mixtures. Some of these materials are in their natural state and they can also be used to improve the mechanical performances of cementitious composites. Sheep wool, which is nowadays considered a special waste, can substitute some polymeric fibres to increase the fracture toughness. However, in alkaline environment, wool fibres tend to degrade within a few days after casting, so fibres can lose the reinforcement function of concrete and mortars due to long term durability issues. A series of tests have been performed with the aim of examining the microstructure and measuring the mechanical properties of wool-reinforced pastes made with various types of cement. By linking the results of microstructural analyses with those of the mechanical tests, it is possible to argue that the lower the pH of the paste the larger the efficiency of wool fibres.

Keywords

wool-reinforced paste, microstructure analyses, residual strength, degradation, sustainability, eco-friendly material

INTRODUCTION

Cement based composites require reinforcement due to their brittle nature and low tensile strength compared to compressive strength. Traditional options for providing tensile reinforcement include steel rebar and fibres, primarily because steel is highly compatible with cement-based systems (Şahin and Köksal 2011). However, it has many disadvantages such as high cost, susceptibility to corrosion, heavy weight, and environmental unfriendliness (Mondal et al. 2020).

To provide a sustainable alternative to reinforcements made with steel and other industrial materials (e.g., glass, basalt, polymer, etc.) many new ideas have recently emerged. In particular, natural animal and plant fibres are gaining attention due to their eco-friendliness, annual renewability, and complete recyclability, aligning with the criteria set by green building rating systems and therefore they are frequently used as construction materials. However, despite the wide variety of natural plant fibres, e.g., bamboo, jute, coir, sisal, palm, or coconut leaf, cotton, and hemp (Mondal et al. 2020, Jóźwiak-Niedźwiedzka and Fantilli 2020) capable of working as reinforcement, certain challenges persist: the reduced durability and the weak bonding with the cement matrix (Mondal et al. 2020). Indeed, significant reduction in the long-term mechanical properties of a composite reinforced with natural fibres has been observed (Kaplan et al. 2021, Fantilli and Jóźwiak-Niedźwiedzka 2021, Bui et al. 2021). This is due to the degradation of the incorporated natural fibres in a Portland cement environment.
On the other hand, in an effort to reduce the cost and the CO_2 emissions, cements companies are introducing blended and special cements in the construction market (Kaplan et al. 2021). In the specific case of natural fibres, there is no information on the durability of composites made with these cements (like blended slag cement CEM III, or sulphoaluminate cements) and the biomaterials of the fibres. Enhancing the durability of cement-based composites is particularly crucial when wool fibres is used as reinforcement, given that wool is nowadays a special waste in most of the European Countries. Thus, the use of large content of wool fibres with special cement lets the development of high-performance composites, as well as the reduction of landfill areas, be possible.
To tailor such composites, a quantitative link between the microstructure aspects and the macroscopic mechanical performances of wool fibre-reinforced pastes has to be found. Accordingly, in this paper, after characterizing three types of cement and wool fibres, some sets of fibre-reinforced paste specimens were cast and tested in three-point bending. Due to an extensive analysis on the microstructures of the pastes, it was possible to correlate mechanical results and material properties, and to provide valuable insights for the tailoring of bio-fibre reinforced composites.

EXPERIMENTAL INVESTIGATION

Materials

Three types of cements were used to cast the fibre-reinforced pastes: ground granulated blast furnace slag cement CEM III/B 42.5 N-LH/SR, calcium sulfoaluminate cement (identified by the commercial code SR03), and ordinary Portland cement CEM I 42.5 R (PN-EN 197-1). Table 1 shows the chemical composition and the physical properties of these cements, whereas the results of isothermal calorimetry are reported in Fig.1.
Calcium sulfoaluminate cement SR03 was characterized by two main hydration peaks which occurred at 5 and 21 min, while cement CEM I and CEM III had one main peak, at 7 and 16 min of hydration, respectively. After 72 h, the total heat of hydration after was 278 J/g for SR03, 288 J/g for CEM I, and 151 J/g for CEM III. In comparison to reference CEM I, SR03 cement reacted faster, and almost of the hydration heat evolution occurred up to 15 hours of hydration, which is a little bit more than that reported by Zhang and Glasser (2002). The heat flow of the subsequent peaks (one or two) for SR03 cement exhibited much higher values than

Portland cement CEM I and slag cement CEM III. The maximum peak for SR03 was more than twice higher than CEM I, and seven times greater than slag cement (35, 15, and 5 mW/g, respectively).

Table 1. Chemical composition and physical properties of the cements used in this research project (XRF method)

Constituent	CEM I	CEM III	SR03
SiO_2 (w/w %)	20.3	28.3	8.7
Al_2O_3 (w/w %)	5.2	7.2	27.5
Fe_2O_3 (w/w %)	3.5	3.6	0.0
CaO (w/w %)	65.3	50.9	43.3
MgO (w/w %)	1.2	4.8	0.9
SO_3 (w/w %)	1.7	2.3	16.9
Na_2O_{eq} (w/w %)	0.6	0.4	0.2
LOI (w/w %)	2.07	2.50	2.30
Blaine specific surface area (cm^2/g)	3800	5300	4100
Density (kg/m^3)	3.15	2.92	2.80

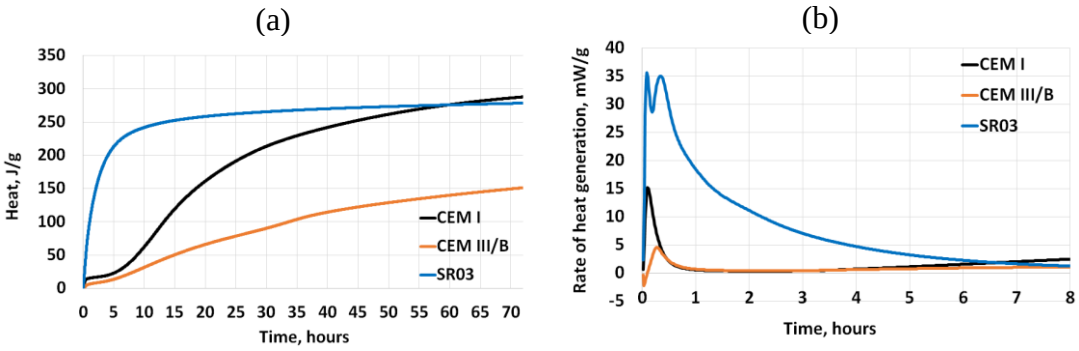

Fig.1 — Results of the isothermal calorimetry: (a) heat of hydration of cements; and (b) the rate of heat generated per 1 g of cement during the first hours hydration.

The XRD analysis also revealed differences in the mineralogical composition of the cements (see Fig.2). In particular, calcium sulphoaluminate cement SR03 differs from those of ordinary Portland and slag cement, because it contains significant amounts of sulphates. On the contrary, CEM I and CEM III were characterized by similar composition, mostly alite and belite, whereas calcium sulphoaluminate cement was mainly composed of yeelimite, anhydrite, Al-rich ferrite, and belite. According to Fig.2, yeelimite and anhydrite corresponding to the rays at 23.7 and 25.5 degrees (2θ), whereas the characteristic weak peak at 32.1 degrees (2θ) confirmed the presence of belite. CEM I also consisted of tricalcium aluminate (C_3A), brownmillerite and gypsum. The C_3A content in the Portland cement is important as it liberates a lot of heat during the early stages of hydration. However, SR03 cement paste harden through the formation of an initial ettringite skeleton, and its subsequent infilling by mixtures of ettringite, calcium monosulphoaluminate hydrate, alumina, and ferrite gel (Zhang and Glasser 2002), which is accompanied by rapid heat release (as shown in Fig.1).

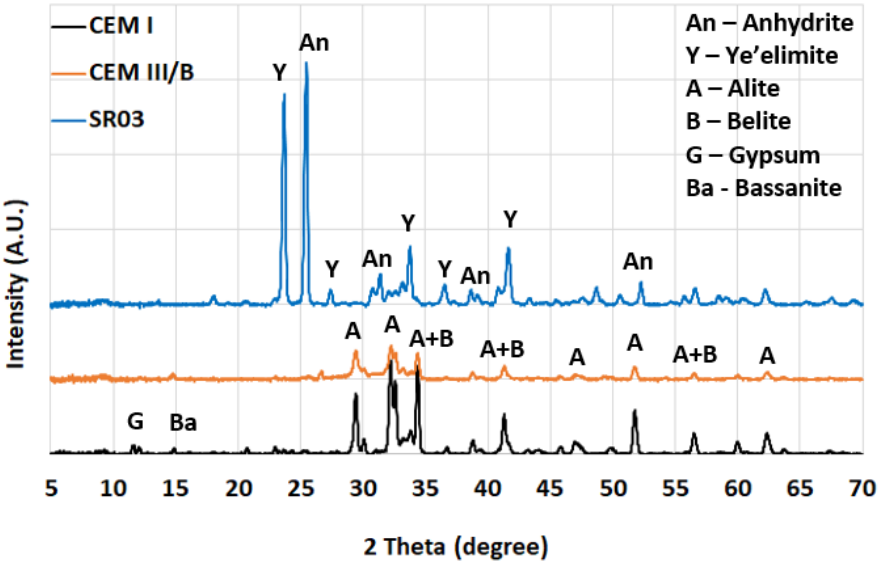

Fig.2 —XRD patterns of cements used in this research project.

The pH of these cements was measured by following the procedure suggested by (Zhang et al. 2020). Namely, 10 g of cement was added to 100 g of distilled water contained into a polyethylene cylinder, which was sealed and properly agitated. After the settlements of the solid particles, the pH was measured with a tester having an accuracy of 0.01 pH. The results of the tests, as presented in Table 2, were measured in a laboratory where the temperature was set to 25±1 °C.

Table 2. The result of pH determination in the three types of cement

CEM I	CEM III	SR03
12.52	12.34	11.12

In each cement past composite, a constant water/binder ratio (equal to 0.5) was maintained. Sheep wool fibres, having a density of 1.0 g/cm^3, an average diameter of 20 μm and an average length of 16 mm, were used in the amount of 2.5% in volume to reinforce the specimens. Detailed characterization of the sheep wool fibres was presented in (Jóźwiak-Niedźwiedzka and Fantilli 2020).
Three prisms (40 × 40 × 160 mm^3) for each composite were cast in order to perform mechanical tests and, subsequently, microstructural analyses. All the specimens were cured in water at the temperature of 20±1°C for 28 days before testing.

Testing procedures and characterization techniques

Three-point bending tests were performed on each specimen following the procedure suggested by EN 196-1 (2016). As shown in Fig.3, the load *P* was applied, through a loading machine with capacity of 500 kN, in the midspan of the specimen, by increasing the midspan deflection η at a velocity of 0.06 mm per minute During the tests, both *P* and η were measured till the complete failure of the specimen.

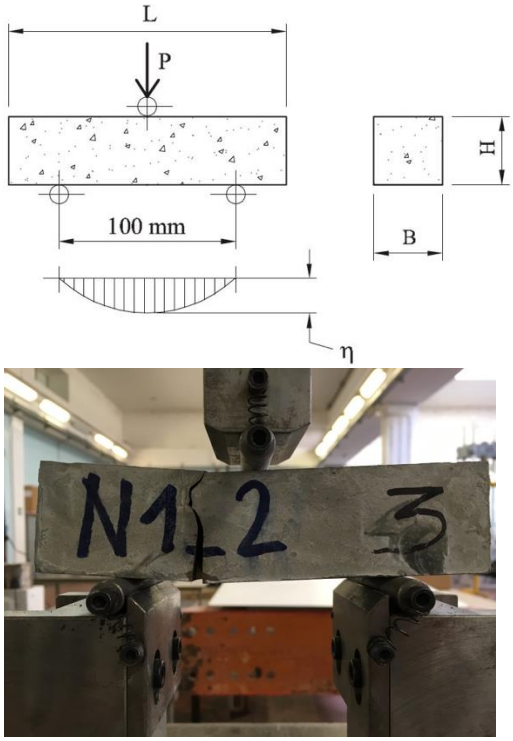

Fig.3 — Three-point bending test on wool-reinforced paste specimen.

Evaluation of the microstructure was performed using a scanning electron microscope (SEM) in the secondary electrons (SE). The morphological characteristic of fibre-reinforced pastes has been investigated on fresh split surface using JEOL JSM-6460 LV high vacuum SEM. The specimens were coated with carbon and a strip of conductive tape was attached to each specimen. A voltage of 15 kV and an aperture of 120 μm were used, whereas the working distance was 9-11 mm. The observations were made using a magnification range of 30× to 1500×.

RESULTS

Mechanical properties

Fig.4a shows the typical load-deflection diagram P-η of the three-point bending tests performed on each specimen. Before the peak of the load, which occurs at $P = P_{max}$ and $\eta = \eta_p$ (the values of P_{max} and η_p are reported in Table 3), an almost monotonic ascending branch can be observed. In this first stage, the paste is uncracked, and fibres do not give any contribution to the strength of the fibre-reinforced composite. On the contrary, after the peak of load (i.e., for $\eta > \eta_p$) crack occurs and the load P rapidly decreases. Afterwards, due to the bridging effect of the fibres, the residual strength remained more or less constant.
As the post cracking stage of the three-point bending tests can be assumed to be the indicator of the fibre efficiency, the post-peak branch of the P- η diagram can be better illustrated with the P-x curve depicted in Fig.4b. In this curve, x represents the difference between the post-peak deflection and the deflection at peak η_p.
Fig.5 shows the P-x curves obtained for all the specimens of each fibre-reinforced composite. It is possible to observe that within the range $0 < x < 2$ mm, the load P remains relatively constant for all the types of fibre-reinforced paste, even if the values of the residual loads depend on the type of cement. Indeed, the highest

residual strength was observed in the case of sulphoaluminate cement, while the highest P_{max} values were registered in the case of CEM III (see Table 3).

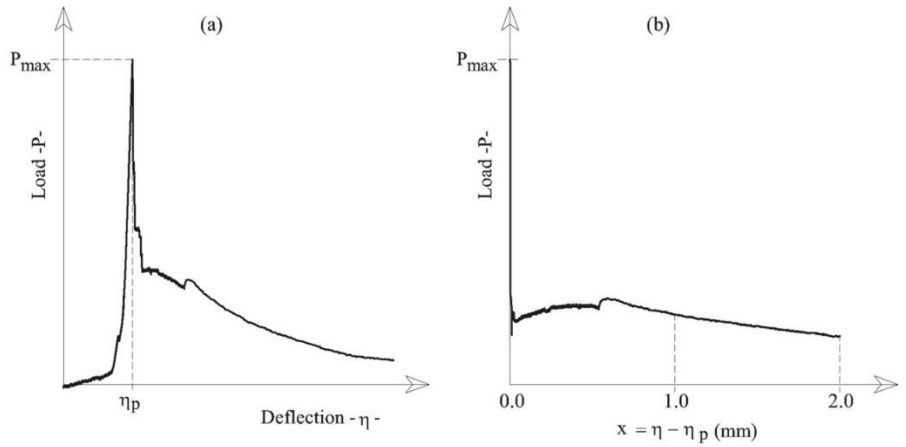

Fig.4 — The results of three-point bending test: (a) ideal load *P*- deflection η diagram; and (b) definition of the post-peak response.

Table 3. Results of the three-point bending tests

Fibre-reinforced paste	Specimen	*B* (mm)	*H* (mm)	P_{max} (N)	η_p (mm)	σ_f (MPa)
CEM I	1	39.98	39.82	276	0.203	0.653
	2	39.68	40.20	241	0.487	0.564
	3	39.70	39.94	296	0.186	0.702
SR03	1	42.90	40.10	381	0.636	0.828
	2	41.92	40.02	452	0.402	1.010
	3	42.28	39.96	348	0.645	0.773
CEM III	1	40.50	39.99	500	0.139	1.159
	2	41.41	40.10	625	0.399	1.408
	3	41.59	40.09	591	0.639	1.327

Microstructure features

Detailed microscopic analysis was conducted on fresh split surface to avoid the influence of carbonation. Figs.6-8 displays the microstructure of hydrated cements in the analysed pastes after 28 days of hydration. A dense microstructure is observed, except in the vicinity of the sheep wool fibres. The SEM analysis revealed that it is possible to distinguish the cement matrix from the zone originally containing the fibres in the CEM I paste, although this zone is characterized by an increased porosity and a complete absence of fibres.

The cement CEM I matrix is primarily composed of dense calcium silicate hydrate (C-S-H), whereas the area previously occupied by the sheep wool fibres is made of thin portlandite tablets containing smaller amounts of potassium, sulphur, and traces of silicon (Fig.6). Within the cementitious matrix, unhydrated slag particles are visible with the fibres in the slag cement matrix, which are only partially present with a predominance of empty spaces (Fig.7).

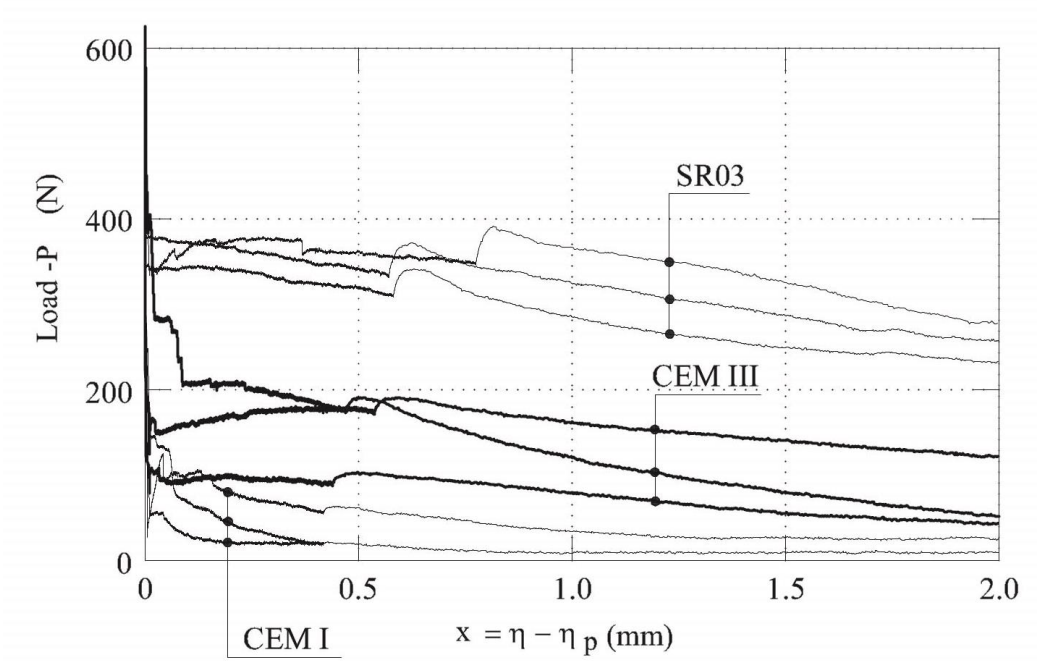

Fig.5. The post-peak response of the wool-reinforced paste tested in this research project.

It is clearly evident that they have undergone partial or superficial degradation. Fig.8 shows the cement matrix SR03, which is composed of monosulfate (AFm) and ettringite (AFt). The cement matrix built from hexagonal AFt crystals is visible, whereas thin-layered AFm crystals can be found in the air voids. Both these minerals play a significant role in the processes of hydration, and contribute to the properties of cement, affecting its strength and various physical characteristics (Aranda and De la Torre 2013).

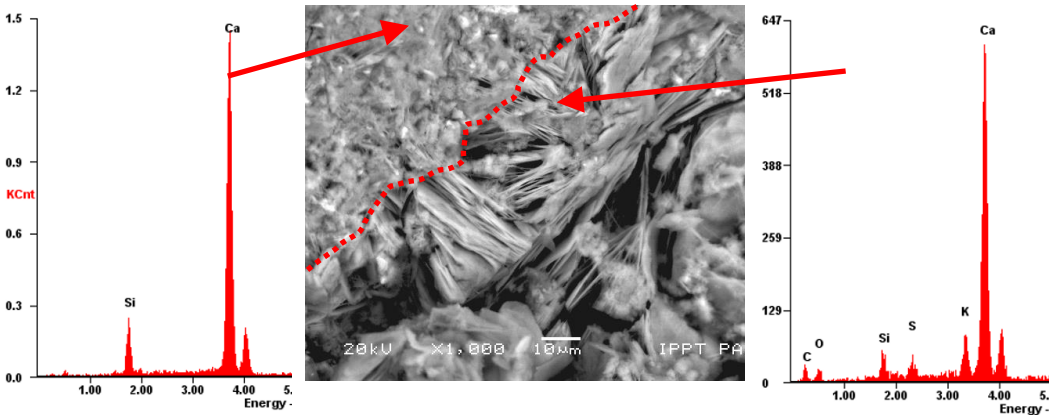

Fig.6 — SEM-EDS microphotograph of paste with CEM I, focusing on the zone between cement matrix and the place where the sheep wool fibres were originally situated (scale bar 10µm).

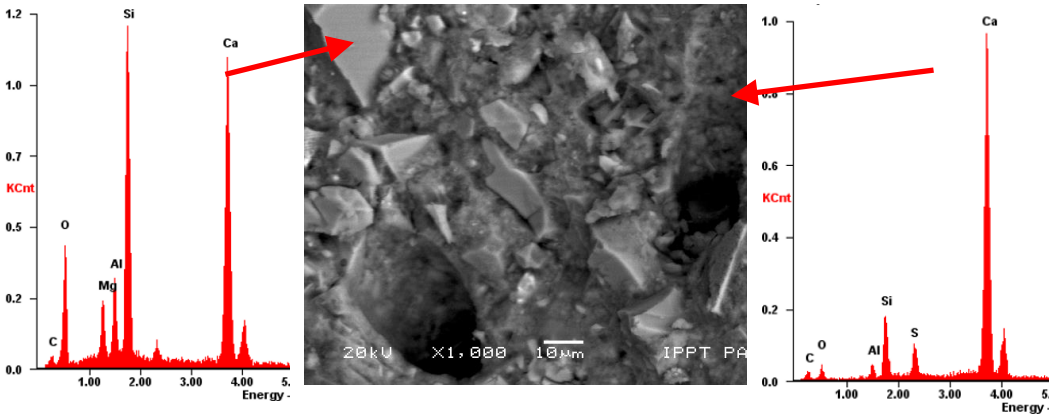

Fig.7 — SEM-EDS microphotograph of paste with CEM III, focusing on empty spaces after the sheep wool fibres degradation, with visible angular slag particles in a cement matrix (scale bar 10µm).

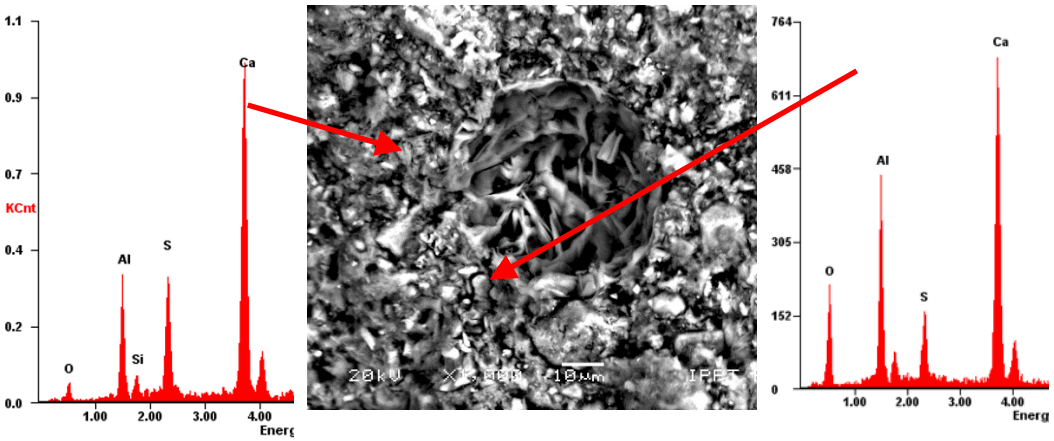

Fig.8 — SEM-EDS microphotograph of paste with SR03, focusing on cement matrix with ettringite and an air-void filled with monosulfate (scale bar 10µm).

DISCUSSION

The different values of pH (Table 2) are clearly reflected in the extent of wool degradation in the fibre-reinforced pastes. Sheep wool fibres degraded in each type of cement matrix, with the most significant damage observed in the reference CEM I matrix, and the least in the SR03 matrix. This observation is supported by the microscopic analysis presented in Fig.9. During the hydration of cements, various hydration products form, including ettringite, which can generate expansive forces, potentially subjecting the wool fibres to mechanical stress and contributing to their degradation (Aranda and De la Torre 2013). However, in this particular case, it appears that the pH level played a crucial role. The elevated pH of the paste can trigger the hydrolysis of the protein-based sheep wool fibres, leading to their gradual deterioration over time. Although Antico et al. (2021) did not observe any fibre degradation process when using pig-hair fibres and Portland-pozzolan cement. As show in Fig.9a, a wool fibre (having an initial diameter d_1 and area A_1) surrounded by the cement-based matrix is damaged, thus the resisting cross-section of the wool reduces (d_2 and A_2 are the final diameter and area of the fibre,

respectively). This pattern of the wool fibre damage is visible in all the three fibre-reinforced pastes (see Fig.9b for CEM I, Fig.9c for CEM III, and Fig.9d for SR03). It is interesting to compare the average values of the ratio A_2/A_1 as determined from 50 observations on each composite. These values, reported in the histogram of Fig.10a, exhibit a correlation with the pH reported in Table 2: a higher pH corresponds to a lower A_2/A_1 ratio. Such an observation confirms the results already obtained by Jóźwiak-Niedźwiedzka and Fantilli (2020), Fantilli and Jóźwiak-Niedźwiedzka (2021), who observed a greater destruction of the sheep wool fibres in high alkaline cement matrix.

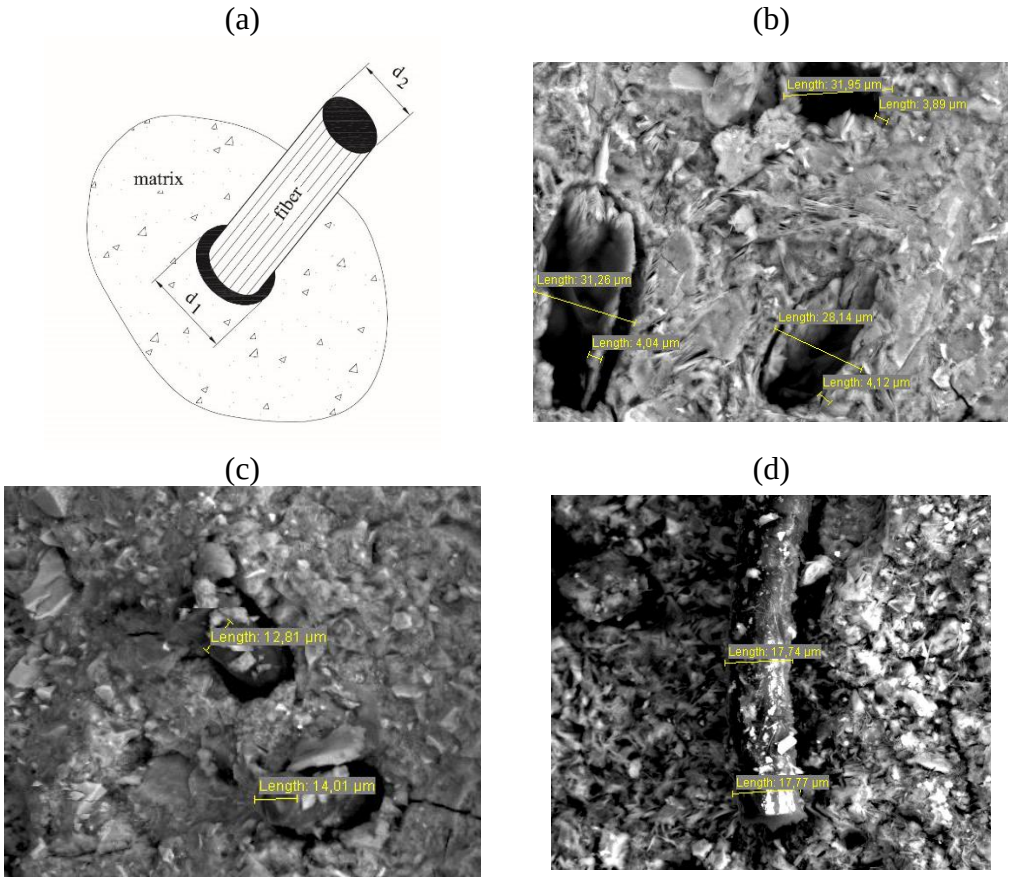

Fig.9 — (a) pattern of the wool fibre degradation; (b) SEM microstructure of paste CEM I; (c) SEM microstructure of paste CEM III; and (d) SEM microstructure of paste SR03.

From a mechanical point of view, this degradation does not affect the flexural strength σ_f of the fibre-reinforced pastes, which is measured as:

$$\sigma_f = \frac{3}{2}\frac{P_{max}\,(100\ mm)}{B\,H^2} \tag{1}$$

where B, H, and P_{max} are the parameters experimentally measured and reported in Table 3. The last column of this Table also contains all the values of σ_f , whereas the histogram of Fig.10b reports the average values of σ_f per each type of wool-reinforced paste. The degradation of the fibres, measured with the ratio A_2/A_1 (Fig.10a), does not match the values of the flexural strength of the pastes (Fig.10b),

which seems to be a function of the cement strength, rather than of the fibre reinforcement.

If P_{max} is substituted by the values of P when x = 1 mm, Eq.1 can be also used to measure the residual strength of the wool reinforced pastes, which mainly depends on the fibre bridging phenomenon across the cracks. The average values of this strength, reported in the histogram of Fig.10c can be linked with the microstructure aspect (i.e., A_2/A_1 of Fig.10a), which in turn depends on the pH of the cement.

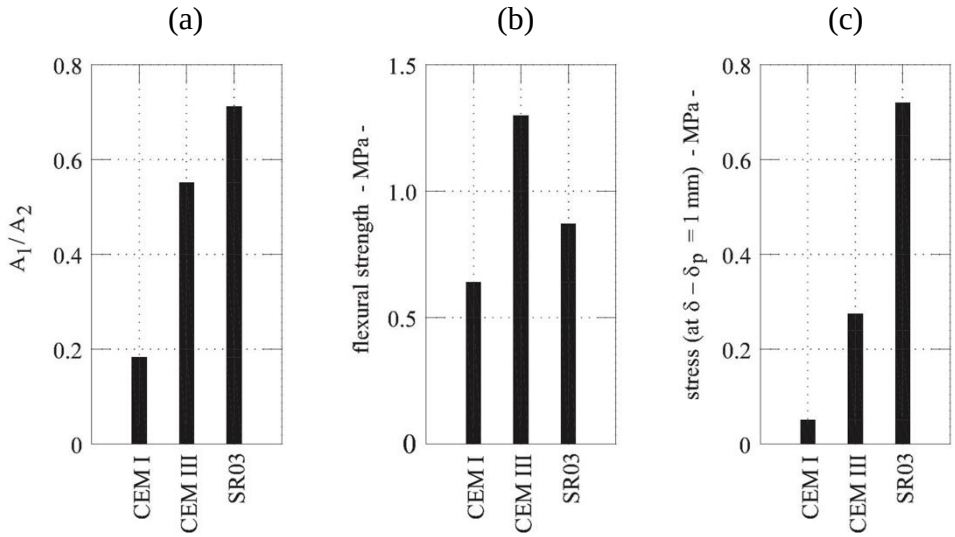

Fig.10 — The average results of the mechanical and micromechanical analyses as a function of the type of cement paste: (a) ratio A_2/A_1; (b) flexural strength; and (c) residual flexural strength after cracking.

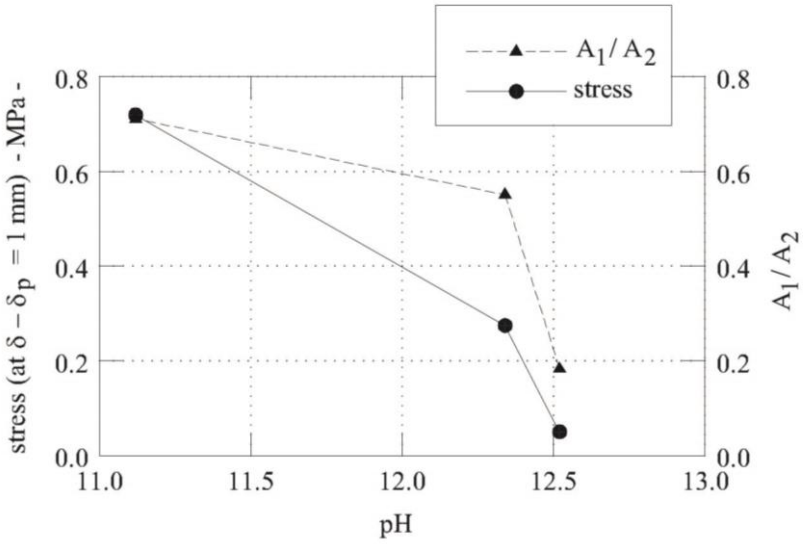

Fig.11 — Residual strength and fibre degradation as a function of the cement pH.

Accordingly, the relationship between cement alkalinity, residual strength, and fibre degradation are summarised in Fig.11, where both the post-peak residual strength and the A_2/A_1 ratio are functions of pH. When the pH of cement exceeds 11.5, a significant damage to the wool fibre is observed, and, consequently, the beneficial effect of the fibre-reinforcement (i.e., the post-cracking residual strength)

drastically reduces. Thus, fibre-reinforced composites made with wool (which is a waste material) and SR03 cement (which is also a low-carbon environmental-friendly binder) can be considered a highly sustainable material to be used in the construction industry.

CONCLUSIONS

The results of the experimental investigations described in the previous sections can be summarized with the following points:

1. When the type of cement varies, pH and the microstructures of wool-reinforced matrix vary as well.
2. The degradation of sheep wool fibres in the cement matrix is solely influenced by the pH of the cements, rather than the strength of the matrix.
3. Indeed, pH does not affect the maximum load in bending before the cracking, but only the residual strength after cracking.
4. In cases where the pH of a cement-based matrix remains below 11.5, as seen in sulphoaluminate cement, the degradation of wool is approximately 30%, which is significantly lower than in CEM I paste, where it reaches 80%.

ACKNOLEDGEMENT

The authors wish to thank Buzzi Unicem s.r.l. for the technical support given to perform the experimental program described in this paper.

REFERENCES

Antico F.C., Rojas P., Briones F., Araya-Letelier G. (2021) “Animal fibers as water reservoirs for internal curing of mortars and their limits caused by fiber clustering”. *Constr Build Mater*, 267, 120918.

Aranda M. A. G., De la Torre A.G. (2013). “Sulfoaluminate cement”, Chapter 18 in Eco-efficient concrete, Woodhead Publishing Limited, 488-522, DOI: 10.1533/9780857098993.4.488

Bui, H., Boutouil, M., Levacher, D., and Sebaibi, N. (2021). “Evaluation of the influence of accelerated carbonation on the microstructure and mechanical characteristics of coconut fibre-reinforced cementitious matrix”. *J. Build. Eng*. 39,102269,1-11.

EN 196-1:2016-07, Methods of testing cement. Determination of strength, (2016),1-33.

Fantilli A.P., and Jóźwiak-Niedźwiedzka D. (2021). “Influence of Portland cement alkalinity on wool reinforced mortar”. *Proc. Inst. Civ. Eng.: Constr. Mater.* 74(3),172-181, 2021.

Jóźwiak-Niedźwiedzka, D. and Fantilli, A.P. (2020). “Wool-reinforced cement-based composites”. *Mater.* 13(16), 3590,1-13.

Kaplan, G., Coskan, U., Benli, A., Bayraktar, O.Y., and Kucukbaltacı, A.B. (2021). “The impact of natural and calcined zeolites on the mechanical and durability characteristics of glass fiber reinforced cement composites”. *Constr Build Mater*. 311,125336,1-19.

Mondal, B., Maity, D. and Patra, P.K. (2020). “Tensile characterisation of bamboo strips for potential use in reinforced concrete members: experimental and numerical study”. *Mater Struct.* 53(128),1-15.

Şahin, Y. and Köksal F. (2011). “The influences of matrix and steel fibre tensile strengths on the fracture energy of high-strength concrete”, *Constr Build Mater*. 25(4),1801-1806.

Zhang, L., and Glasser, F.P. (2002). “Hydration of calcium sulfoaluminate cement at less than 24 h”. *Adv. Cem. Res.* 14(4),141-155.

Zhang, J., Guan, X., Wang, X., Ma, X., Li, Z., Xu, Z., and Jin, B. (2020). “Microstructure and properties of sulfoaluminate cement-based grouting materials: effect of calcium sulfate variety”. *Adv. Mater. Sci. Eng*. 7564108.

SCMT

Sustainable Construction Materials and Technologies

6

PROCEEDINGS OF THE SIXTH INTERNATIONAL CONFERENCE ON SUSTAINABLE CONSTRUCTION MATERIALS AND TECHNOLOGIES

Volume I

Lyon, France

June 9th – 13th 2024

Editors

Nader Ghafoori

Eshmaiel Ganjian

Jean-Claude Morel

Antonin Fabbri

Morteza Khorami

6th International Conference on Sustainable Construction Materials and Technologies

SCMT 6
Sustainable Construction Materials and Technologies

9TH – 13TH June 2024

Lyon, France

Proceedings

Volume 1

Editors:

Nader Ghafoori
Eshmaiel Ganjian
Jean-Claude Morel
Antonin Fabbri
Morteza Khorami

River Soane in Central Lyon, France
Photo by L.V./Lyon Tourism and Congre

Table of Contents

Volume 2

June 9th – 13th 2024

Lyon, France

The SCMT6 Proceedings, compiled in two volumes, feature 84 technical articles from 30 countries that were presented during the conference. This collection of articles represents the latest research and development in different construction materials with emphasis on innovation, durability, sustainability, and efficiency

ISBN 9798332048715